

# Propagation characteristics of plasma sheet oscillations during a small storm

C. Gabrielse (1), V. Angelopoulos (1), A. Runov (1), L. Kepko (2), K. H. Glassmeier (3),

U. Auster (3), J. McFadden (4), C. W. Carlson (4), D. Larson (4)

(1) IGPP/UCLA; (2) UNH; (3) TUBS; (4) SSL/UCB

## Abstract

On 24 March 2007, the THEMIS spacecraft were in a string-of-pearls configuration through the dusk plasma sheet at the recovery phase of a small storm. Large undulations of the plasma sheet were observed that brought the five probes from one lobe to another. Each neutral sheet crossing was accompanied by bursty bulk flows and Pi2 oscillations. In this paper we focus on the low frequency (~10 min) large scale plasma sheet undulations and determine their propagation characteristics, origin, and properties in the presence of storm-time substorms. As the first case of “flapping waves” observed and analyzed during storm-time, it is interesting to find their characteristics coincide with those described by previous quiet-time observations. These characteristics include flankward propagation of the undulations with velocities generally between ~40-130 km/s.

## 1. Introduction

Flapping waves are large scale magnetic field variations observed in the magnetotail plasma sheet with amplitude of several tens of nT and a characteristic time scale of several to ten minutes. Recent multi-point observations with the Cluster spacecraft (apogee at  $R = -19 R_E$ ) have shown that flapping is due to solitary kinks of the current sheet propagating flankward from the near-midnight region of the magnetotail rather than an up-down motion of the entire plasma sheet [Sergeev et al., 2004, Runov et al., 2005]. Applying the four-point timing analysis [Harvey, 1998] to about a hundred of the current sheet crossings (marked by a change of the  $B_x$  sign) by the Cluster quartet, Runov et al. [2005] have found that i) the GSM x- and y-components of the normal to a front velocity of flapping waves ( $V_n$ ) are, generally, positive and negative ( $V_{n_x} > 0$ ,  $V_{n_y} < 0$ ) in the dawn sector, while both are positive ( $V_{n_x} > 0$ ,  $V_{n_y} > 0$ ) in the dusk sector of the plasma sheet; ii) the xy GSM projections of  $V_n$  are, generally, perpendicular to the flaring magnetic field (direction of maximum variance); and iii) the velocity value occurrence rate distribution is double-peaked with maxima at  $\sim 50$  and at  $\sim 150$  km/s.

Simultaneous observations of a set of rapid current sheet crossings by Cluster and Double Star TC-1 spacecraft, aligned in local time in the dawn sector and separated radially by about  $6 R_E$ , showed that flapping waves are radially elongated, forming folds of the current sheet and propagating flankward with respect to the spacecraft [Zhang et al., 2005]. In comparison, in another study [Volwerk, 2007], the four-point timing analysis was applied to Kelvin-Helmholtz waves with a period of  $\sim 5$  minutes. These were determined to propagate mainly Earthward with a phase velocity of  $\sim 250$  km/s.

Statistical analysis of hundreds of the current sheet crossings by the Geotail spacecraft reveals that the occurrence rate of flapping is similar to that of bursty bulk flows [Sergeev et al., 2006].

The physical mechanism of flapping wave excitation and its relation to the bursty bulk flows (BBFs) is not yet established. Some theoretical concepts imply a ballooning-like mode oscillation in the high-beta plasma sheet with a large normal component of the magnetic field [Golovchanskaya and Maltsev, 2004]. Recently, Erkaev et al. [2007] have shown that the flapping waves may be excited if the gradients of the tangential and normal magnetic field along the normal ( $\partial_n B_t$ ) and tangential ( $\partial_t B_n$ ) directions with respect to the current sheet exceed some threshold. In their paper the authors assume that such a situation is indeed realized by BBFs.

THEMIS is a five identically-instrumented satellite mission launched in February of 2007 with the primary objective of studying the magnetosphere's activity while aligned at  $\sim 10$ , 20, and 30  $R_E$  (with ground magnetometers) to judge between the two existing models of substorm evolution [see Angelopoulos et al, 2008]. Before reaching this configuration, the spacecraft were in a string of pearls (see Figure 1), making our observations and analyses on 24 March 2007 possible. The onboard instrumentation includes electric field instruments (EFI), fluxgate magnetometers (FGM), search coil magnetometers (SCM), electrostatic analyzers (ESA), and solid state telescopes (SST). In our analyses we used the FGM [Auster et al., 2008] data to measure the magnetic field and the ESA [McFadden et al., 2008] to measure the particle velocities (obtained from onboard

moments). The THEMIS mission also incorporates 20 ground-based magnetometers which we used to determine the AE index [Mende et al., 2008]. We used filtered data (5-140 seconds) from the station at UKIA to portray the Pi2 pulsations during the time of interest.

The THEMIS mission gives an opportunity to probe the magnetotail plasma/current sheet on a global scale, providing simultaneous measurements at five identical spacecraft separated by distances varying from about 0.1 to 2  $R_E$  (see Figure 1) during our time interval of interest. Having a larger spatial separation than Cluster, THEMIS is more suited for studying the evolution from one structure to another. In this letter we discuss the THEMIS observations of the equatorial near-Earth plasma sheet in the dusk-side sector at geocentric distances less than 15  $R_E$  during a storm-time substorm (Dst index was -70 nT, see also Figure 2 for AE index). The flapping waves we observed on 24 March 2007 between 9:00 and 9:40 UT, plotted in the Bx component in Figure 2, have a low frequency (period of about 10 minutes) and large spacing, which allows us to determine the propagation speed.

The case we investigate in this paper is especially interesting because the flapping waves were observed in association with their potential generators, i.e. BBFs, which has not been observed before. Furthermore, this flapping motion has not been well studied in the dusk region of the plasma sheet at such small radial distances ( $R \approx 14.7 R_E$ ). During this time interval, LANL-97 (which was also in the dusk sector at about 6  $R_E$ ) observed particle injections that are time-correlated with the flapping waves. (Not shown, see

[http://leadbelly.lanl.gov/lanl\\_ep\\_data/.](http://leadbelly.lanl.gov/lanl_ep_data/)) We also note that the AE index increases when Bz turns southward (both plotted in Figure 2).

## 2. Data Analysis

In our study, we use a similar timing method as used for Cluster through triangulation of the THEMIS spacecraft in order to determine the waves' propagation velocity and to compare the propagation direction to the direction of maximum variance. We applied this also to find the front speed of the x-component of the particle velocities ( $V_{Vx}$ ) as measured by the five THEMIS spacecraft.

From Cluster we know that the perturbation is in the equatorial plane, propagating duskward in the dusk sector and dawnward in the dawn sector. THEMIS has much greater distances between spacecraft in the equatorial plane than Cluster, thus we were interested in probing these large flapping structures with a three-point timing system (using the leading, trailing, and one middle spacecraft) to measure their propagation velocities on the equatorial plane. These combinations gave three data points per event: THEMIS CAE, CBE, and CDE.

The time lag between spacecraft was determined using a maximum correlation method for the first four neutral sheet crossings we studied (see Figure 3), described as:

$$\sum \sqrt{\frac{[th_1(i) - th_2(i - \tau)]^2}{N}} \quad (1)$$

where the two functions (each function being the Bx data of one spacecraft) are best correlated when the sum is at a minimum.

The spacecraft's physical location was chosen when the Bx data was at a max, since that is an obvious point in the information and we are confident it is the same data traversed from one spacecraft to the next. It can also be noted—and seen in Figure 1—that the spacecraft do not physically move in their orbit much at all from one peak to another, making any positional error essentially negligible. This also implies that the calculated propagation velocities would not be affected by the spacecrafts' velocities. It should be noted when viewing the intervals in Figure 2 that the first 70 seconds, approximately, were not included in the correlation itself, but were necessary to run the maximum correlation through  $\tau = 70$  seconds.

The timing analysis to determine  $V_{v_x}$  and the direction of the x-component of the velocity data (second to last panel in Figure 2) was the same as above—[Harvey, 1998] applied to three instead of four spacecraft—except that the time lag was calculated differently. The velocity data was not as identical from one spacecraft to the other and thus the maximum correlation method could not be used. Instead we chose a point in a data set (such as a maximum or minimum) where it was apparent in the other data sets as well, and found the time difference between those points. There was no adequate correlation between the spacecraft during the final time interval, which is why Figure 3 is lacking a black arrow. This method was also used to find the time lag for the final

neutral sheet crossing, as the maximum correlation method does not work in this case either.

In Figure 3 we see the directions of the maximum variance of Bx (blue) and the propagation directions of the waves (red). The maximum variance direction that corresponded to the best (biggest) eigenvalue ratio out of the three possible triangles was used for each interval. The Bx propagation direction is an average between the three triangles' measurements (CAE, CBE, CDE) since the variance was slight for all but the final interval. The ranges of these angles (measured from the +x-axis) are 21 to 23, 29 to 30, -23 to -27, 22 to 27, and -20 to -50 degrees, for each respective interval. We can postulate that the last varied by so much due to the less rigorous timing method we had to use.

As we can see, unlike Cluster's results, the propagation direction and the direction of maximum variance are not exactly perpendicular. However, the Runov et. al [2005] paper incorporated 80 events, and as we are looking at a single case we can maintain that the analyses are in agreement. The propagation directions of the particle velocity waves are also plotted in Figure 3 (black). The angles from the triangles we used were again typically within a few degrees of each other. We see an association with the flapping waves' and the particle velocities' propagation directions. The velocity ranges in Figure 3 represent the range of propagation velocities determined by using the three triangles. This gives us a sense of the error. As the Cluster observations demonstrated that the velocity value occurrence rate distribution is double-peaked with maxima at ~50 and at

~150 km/s, our results demonstrate a good correlation since all but one of our measurements were within ~40-130 km/s. The one case that measured ~250 km/s propagation speed was not, however, unlike any of the Cluster observations.

In three of the five cases the flapping waves are propagating flankward, while in two cases they are traveling slightly Earthward. These two cases were measured during the wave's max peak to min peak intervals, while the three were measured during the min to max intervals. (We were unable to correlate the Bx max to min interval at 9:13-9:15.) All cases have a larger positive x-component (sunward) than y-component, which aligns with Cluster's observations since THEMIS was located far out in the flank.

### 3. Conclusion

As the first case ever found and studied of westward traveling plasma sheet undulations—flapping waves—in storm time, we find their properties to be relatively consistent with earlier observations of non-storm time events. The propagation velocity ranges and the general propagation directions we found are concurrent with those measured by Cluster for a dusk sector event. We therefore dismiss the possibility that these are Kelvin-Helmholtz waves, since they have been observed to propagate mainly Earthward with much faster velocities [Volwerk, 2007]. Another example of concurrence with the Cluster-observed flapping waves is that Cluster observed these motions during the substorm expansion phase. Looking at Figure 2, we see that each wave is associated with an increase in the AE index, also demonstrating a substorm correlation.

Previously, the connection between BBFs and flapping waves could only be assumed since statistical signatures indirectly pointed to this association. The occurrence rate of flapping waves has been observed to resemble BBFs'—but this still leaves a lack of direct evidence. We, however, found direct evidence that the flapping waves are linked to fast flows. This evidence is displayed in Figure 2, as each time we detect a BBF, a flapping wave is at onset. Also, observing the Pi2 pulsations at each undulation's onset further indicates that the flapping waves are linked to the BBFs since Pi2 waves are known to be well-correlated to BBFs.

#### Acknowledgements

We acknowledge NASA contract NAS5-02099 for use of data from the THEMIS Mission. Specifically: W. Baumjohann, and with financial support through the German Ministry for Economy and Technology and the German Center for Aviation and Space (DLR) under contract 50 OC 0302. The orbit images were obtained from NASA through the SSCWeb 3D orbital viewer program Tipsod. We would also like to acknowledge the help and advice from the UCLA IGPP programmers.

## References

- Angelopoulos, V. (2008), The THEMIS mission, *Space Sci. Rev.*, 13x, submitted.
- Auster, H. U., et al. (2008), The THEMIS fluxgate magnetometer, *Space Sci. Rev.*, xx, submitted.
- Erkaev, N. V., V. S. Semenov and H. K. Biernat (2007), Magnetic double-gradient instability and flapping waves in a current sheet, *Phys. Rev. Lett.*, 99, 235003.
- Golovchanskaya, I. V. and Y. P. Maltsev (2004), On the identification of plasma sheet flapping waves observed by Cluster, *Geophys. Res. Lett.*, 32, L02102, doi:10.1029/2004GL021552.
- Harvey, C. C. (1998), Spatial gradients and volumetric tensor, in: *Analysis Methods for Multi-Spacecraft Data*, G. Paschmann and P. Daly (Editors), pp. 307–322, ESA, Noordwijk.
- McFadden, J. P., C. W. Carlson, D. Larson, V. Angelopoulos, M. Ludlam, R. Abiad, and B. Elliot (2008), The THEMIS ESA plasma instrument and in-flight calibration, *Space Sci. Rev.*, XX, submitted.
- Mende, S. B., et al (2008), The THEMIS array of ground based observatories for the study of auroral substorms, *Space Sci. Rev.*, 13x, submitted.
- Runov, A., et al. (2005), Electric current and magnetic field geometry in flapping magnetotail current sheets, *Ann. Geophys.*, 23, 1391–1403, 2005.
- Sergeev, V., A. Runov, W. Baumjohann, R. Nakamura, T. L. Zhang, A. Balogh, P. Louarn, J.-A. Sauvaud, and H. Reme (2004), Orientation and propagation of current sheet oscillations, *Geophys. Res. Lett.*, 31, L05807, doi:10.1029/24452003GL019346.

- Sergeev, V. A., D. A. Sormakov, S. V. Apatenkov, W. Baumjohann, R. Nakamura, A. Runov, T. Mukai, and T. Nagai (2006), Survey of large-amplitude flapping motions in the midtail current sheet, *Ann. Geophys.*, 24, 2015–2024.
- Volwerk, M., K.-Glassmeier, R. Nakamura, T. Takada, W. Baumjohann, B. Klecker, H. Rème, T. L. Zhang, E. Lucek, and C. M. Carr (2007), Flow burst-induced Kelvin-Helmholtz waves in the terrestrial magnetotail, *Geophys. Res. Lett.*, 34, L10102, doi:10.1029/2007GL029459.
- Zhang, T. L., et al. (2005), Double Star/Cluster observations of neutral sheet oscillations on 5 August 2004, *Ann. Geophys.*, 23, 2909–2914.

Captions:

Figure 1. SSCWeb 3D Orbit Viewer shows the orbital path of the five THEMIS spacecraft configuration from 9-9:40 UT, paused halfway through at 9:20 UT. The XYZ components are GSM coordinates, and as one can see the spacecraft all lie mostly on the XY-plane.

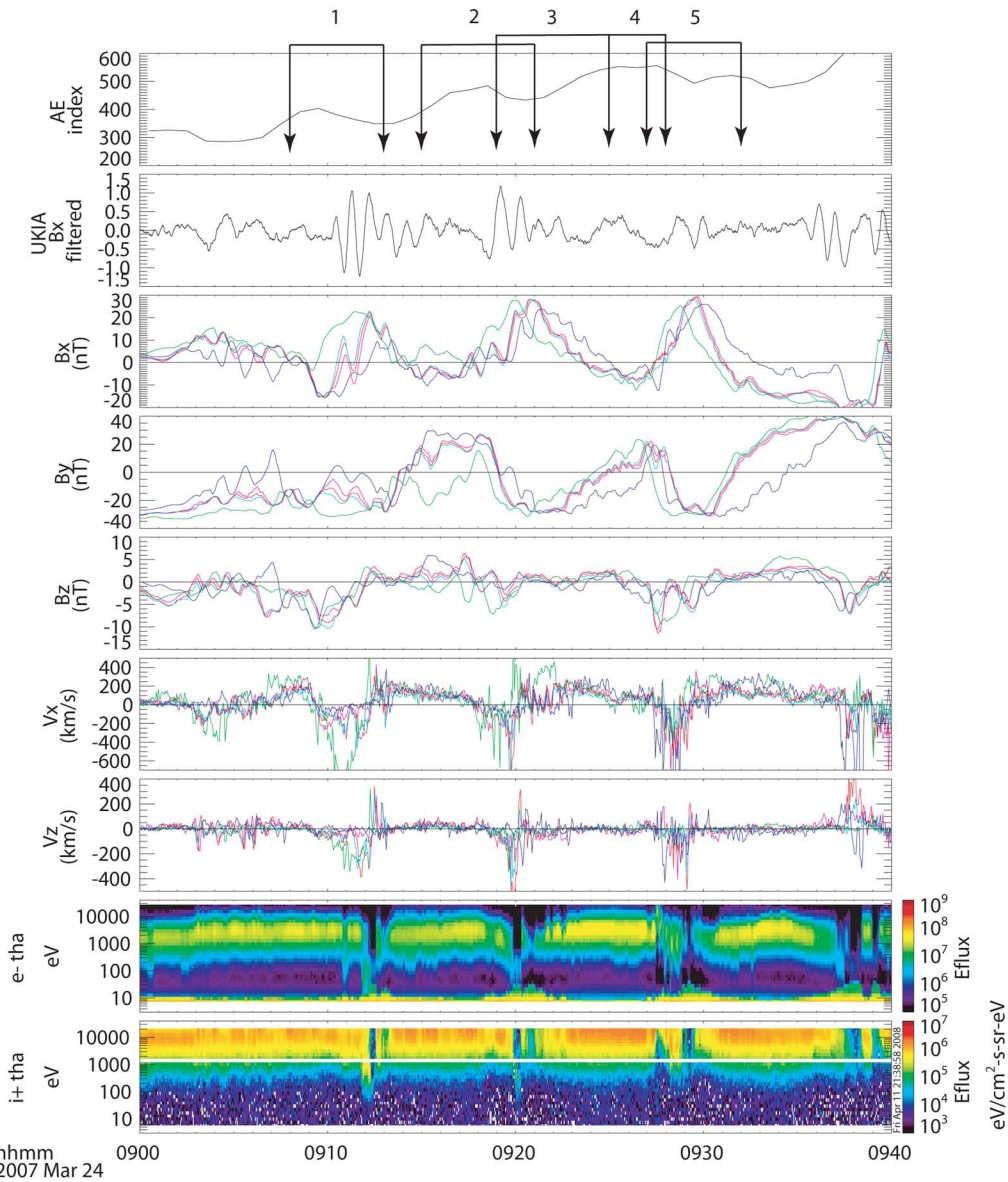
Figure 2. The first two panels are measured by THEMIS ground stations: the AE index in the first panel, the Pi2 pulsations as observed by UKIA in the second. The next three panels exhibit plasma sheet flapping: The x, y, and z-components of the magnetic field, respectively, as measured by THEMIS A (magenta), B (red), C (green), D (cyan), and E (blue). The 6<sup>th</sup> and 7<sup>th</sup> panels show the x- and z-components of the particle velocities measured by THEMIS. (The y- component is unavailable due to an onboard software error that jumbled up the contributions of different angular sectors which affected  $V_y$ .) The last two panels are the ion and electron fluxes as measured by THA, which was the middle spacecraft in the configuration. The arrows (labeled 1-5) point at the start and end of each time interval used (refer to Figure 3).

Figure 3. Each panel represents information we deduced from each min/max to max/min interval. The black dot represents the location of THEMIS B in GSM coordinates. The blue arrow points in the direction of maximum variance. The red arrow points in the propagation direction of the flapping waves. The black arrow points in the propagation direction of the particle velocities. The velocity ranges are the propagation velocity ranges calculated using the timing analysis for the Bx data and the particle velocity ( $V_x$ ) data for each of the three triangles (CAE, CBE, and CDE).



Satellite	Color	X	Y	Z
THEMIS-A (P5)	Magenta	-4.655	13.897	0.115
THEMIS-B (P1)	Red	-4.777	13.865	0.099
THEMIS-C (P2)	Green	-5.831	13.113	-0.088
THEMIS-D (P3)	Cyan	-4.859	13.835	0.084
THEMIS-E (P4)	Blue	-3.482	13.867	0.277

# Overview Plot



hhmm  
2007 Mar 24

